THE JOURNAL OF BIOLOGICAL CHEMISTRY VOL. 290, NO. 14, pp. 8677–8692, April 3, 2015


# A Role for the Tyrosine Kinase Pyk2 in Depolarization-induced Contraction of Vascular Smooth Muscle*◆

Received for publication, December 15, 2014, and in revised form, February 11, 2015 Published, JBC Papers in Press, February 24, 2015, DOI 10.1074/jbc.M114.633107

**Ryan D. Mills**[‡1,2], **Mitsuo Mita**[§1], **Jun-ichi Nakagawa**[§], **Masaru Shoji**[§], **Cindy Sutherland**[‡], **and Michael P. Walsh**[‡3]

*From the* [‡]*Smooth Muscle Research Group, Department of Biochemistry and Molecular Biology, Libin Cardiovascular Institute and Hotchkiss Brain Institute, University of Calgary, Calgary, Alberta T2N 4N1, Canada and the* [§]*Department of Pharmacodynamics, Meiji Pharmaceutical University, 2-522-1 Noshio, Kiyose, Tokyo 204-8588, Japan*

**Background:** Depolarization-induced tonic contraction of vascular smooth muscle involves tyrosine phosphorylation.
**Results:** Depolarization activates the $Ca^{2+}$-dependent tyrosine kinase Pyk2, leading to activation of the RhoA/Rho-associated kinase pathway.
**Conclusion:** Activation of Pyk2 is required for the sustained phase of depolarization-induced contraction.
**Significance:** Knowledge of the mechanisms responsible for sustained contraction is crucial for identification of defects leading to disease associated with vascular contractile dysfunction.

**Depolarization of the vascular smooth muscle cell membrane evokes a rapid (phasic) contractile response followed by a sustained (tonic) contraction. We showed previously that the sustained contraction involves genistein-sensitive tyrosine phosphorylation upstream of the RhoA/Rho-associated kinase (ROK) pathway leading to phosphorylation of MYPT1 (the myosin-targeting subunit of myosin light chain phosphatase (MLCP)) and myosin regulatory light chains ($LC_{20}$). In this study, we addressed the hypothesis that membrane depolarization elicits activation of the $Ca^{2+}$-dependent tyrosine kinase Pyk2 (proline-rich tyrosine kinase 2). Pyk2 was identified as the major tyrosine-phosphorylated protein in response to membrane depolarization. The tonic phase of $K^+$-induced contraction was inhibited by the Pyk2 inhibitor sodium salicylate, which abolished the sustained elevation of $LC_{20}$ phosphorylation. Membrane depolarization induced autophosphorylation (activation) of Pyk2 with a time course that correlated with the sustained contractile response. The Pyk2/focal adhesion kinase (FAK) inhibitor PF-431396 inhibited both phasic and tonic components of the contractile response to $K^+$, Pyk2 autophosphorylation, and $LC_{20}$ phosphorylation but had no effect on the calyculin A (MLCP inhibitor)-induced contraction. Ionomycin, in the presence of extracellular $Ca^{2+}$, elicited a slow, sustained contraction and Pyk2 autophosphorylation, which were blocked by pre-treatment with PF-431396. Furthermore, the $Ca^{2+}$ channel blocker nifedipine inhibited peak and sustained $K^+$-induced force and Pyk2 autophosphorylation. Inhibition of Pyk2 abolished the $K^+$-induced translocation of RhoA to the particulate fraction and the phosphorylation of MYPT1 at Thr-697 and Thr-855. We conclude that depolarization-induced entry of $Ca^{2+}$ activates Pyk2 upstream of the RhoA/ROK pathway, leading to MYPT1 phosphorylation and MLCP inhibition. The resulting sustained elevation of $LC_{20}$ phosphorylation then accounts for the tonic contractile response to membrane depolarization.**

Membrane depolarization evoked by neurotransmitter release is a key mechanism of activation of vascular smooth muscle contraction. Depolarization leads to activation of voltage-gated $Ca^{2+}$ channels, $Ca^{2+}$ entry from the extracellular space, myosin regulatory light chain ($LC_{20}$)[4] phosphorylation by $Ca^{2+}$/calmodulin-dependent myosin light chain kinase (MLCK), and contraction (1, 2). Although this mechanism accounts for the rapid (phasic) contraction elicited by membrane depolarization, this is followed by a sustained (tonic) contraction, which requires activation of the RhoA/Rho-associated kinase (ROK) pathway, leading to inhibition of myosin light chain phosphatase (MLCP) via phosphorylation of MYPT1, the myosin targeting subunit of MLCP (3–5).

It remains unclear, however, how membrane depolarization and $Ca^{2+}$ entry lead to the activation of RhoA. We demonstrated recently that genistein-sensitive tyrosine phosphorylation lies upstream of RhoA activation in response to membrane depolarization, and hypothesized that the $Ca^{2+}$-dependent tyrosine kinase Pyk2 (proline-rich tyrosine kinase 2) may be involved (6). We have addressed this hypothesis in de-endothelialized rat caudal arterial smooth muscle strips using a variety of Pyk2 inhibitors in conjunction with measurements of Pyk2 autophosphorylation (activation), RhoA translocation, and MYPT1 and $LC_{20}$ phosphorylation, and we conclude that Pyk2 is activated in response to depolarization-induced $Ca^{2+}$ entry

* This work was supported by a grant from the Canadian Institutes of Health Research (CIHR MOP-111262) (to M. P. W.) and a grant from the High-Tech Research Center Project, the Ministry of Education, Culture, Sports, Science and Technology (MEXT), Japan (S0801043) (to M. S.).
◆ This article was selected as a Paper of the Week.
[1] Both authors contributed equally to this work.
[2] Recipient of a Kertland Family Postdoctoral Fellowship in Vascular Biology.
[3] Holds a Canada Research Chair (Tier 1) in Vascular Smooth Muscle Research. To whom correspondence should be addressed: Dept. of Biochemistry and Molecular Biology, Cumming School of Medicine, University of Calgary, 3330 Hospital Dr. N.W., Calgary, Alberta T2N 4N1, Canada. Tel.: 403-220-3021; E-mail: walsh@ucalgary.ca.

[4] The abbreviations used are: $LC_{20}$, 20-kDa myosin regulatory light chain subunit; MLCK, myosin light chain kinase; MLCP, myosin light chain phosphatase; MYPT1, myosin light chain phosphatase targeting subunit 1; ROK, Rho-associated kinase; FAK, focal adhesion kinase; pTyr, phosphotyrosine; pThr, phosphothreonine.

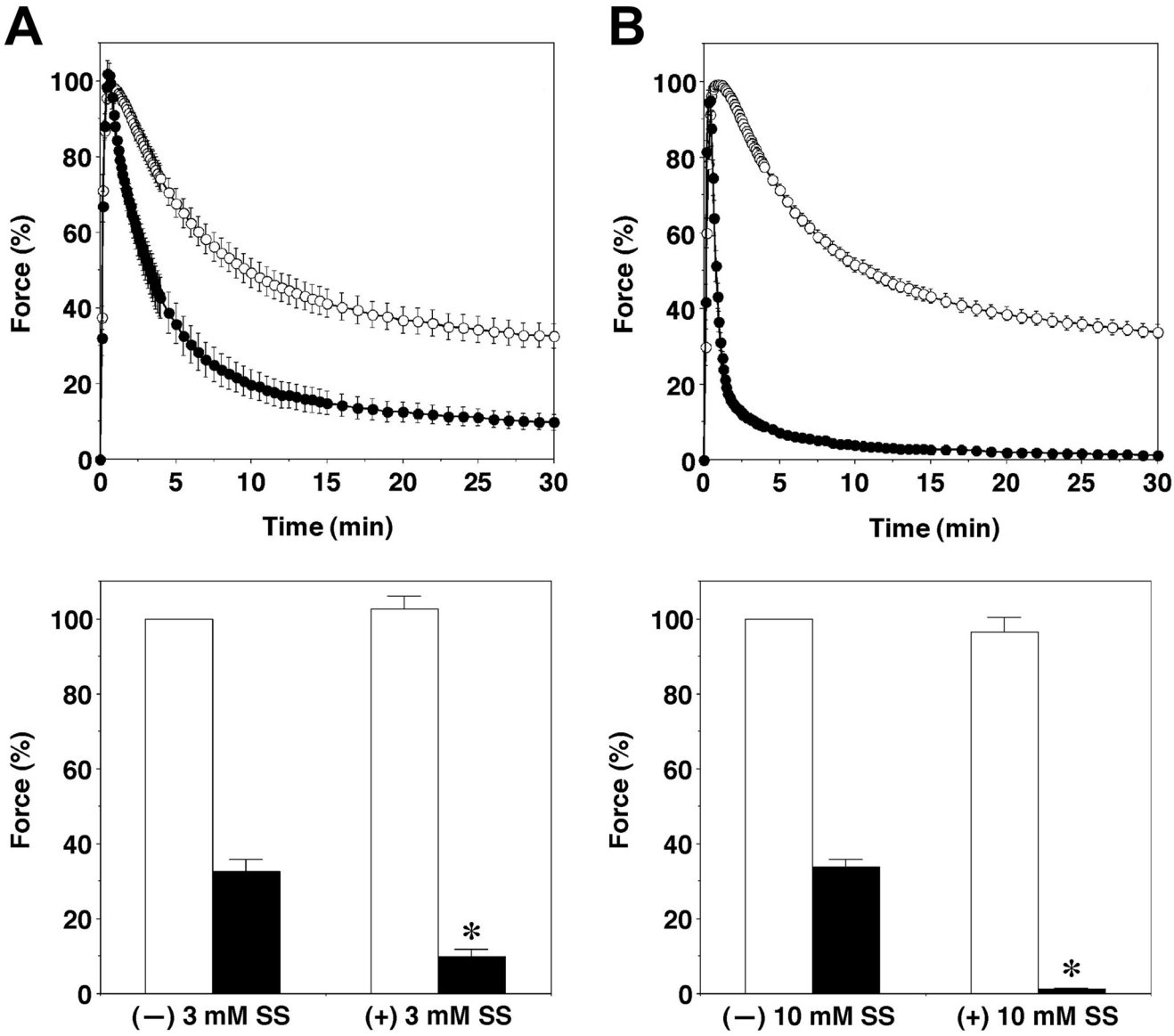


FIGURE 1. **Effect of pre-treatment with sodium salicylate on $K^+$-induced contraction.** *A* and *B*, *upper panels* show the time courses of $K^+$-induced contraction without (○) or with (●) sodium salicylate (*SS*) pre-incubation (3 mM in *A* and 10 mM in *B*). *Lower panels* show the effects of sodium salicylate on the phasic (*open bars*) and tonic (*filled bars*; 30 min after $K^+$ addition) components of $K^+$-induced contraction. Force is expressed as a percentage of the maximal force of the phasic contraction induced by $K^+$ without sodium salicylate. Values represent the mean ± S.E. ($n = 8$). *, $p < 0.001$, significantly different from the value of the force without sodium salicylate.

and lies upstream of RhoA and ROK, leading to MLCP inhibition and sustained contraction.

## EXPERIMENTAL PROCEDURES

*Materials*—Sodium salicylate was purchased from Wako Pure Chemical Industries (Osaka, Japan). PF-431396, PF-573228, and ionomycin were purchased from Sigma. NVP-TAE226 and PF-562271 were purchased from Selleck Chemicals. ML-9, sodium orthovanadate, and calyculin A were purchased from Calbiochem, and FAK inhibitor sc-203950 was purchased from Santa Cruz Biotechnology.

*Force Measurements in Isolated Muscle Strips*—Caudal arteries were removed from male Sprague-Dawley rats (300 – 400 g) after sacrifice using protocols consistent with the standards of the Canadian Council on Animal Care and approved by the Institutional Ethics Committee for Animal Research at Meiji Pharmaceutical University and the University of Calgary Animal Care and Use Committee. De-endothelialized caudal arterial smooth muscle strips were prepared for force measurement as described previously (3, 7). Experiments were carried out with endothelium-denuded vessels to eliminate interference from endothelial cell-derived vasoactive mediators. Tissues were stimulated with 60 or 87 mM KCl by replacing NaCl in Hepes-Tyrode's solution with equimolar KCl. These concentrations of KCl induce close-to-maximal contractile responses: 85.5% at 60 mM and 90.3% at 87 mM KCl.

*Western Blotting*—Tissues were harvested at the times indicated in the figure legends for protein extraction, SDS-PAGE (10% or 7.5% acrylamide), or Phos-tag SDS-PAGE (Wako Pure Chemical Industries) and Western blotting with enhanced

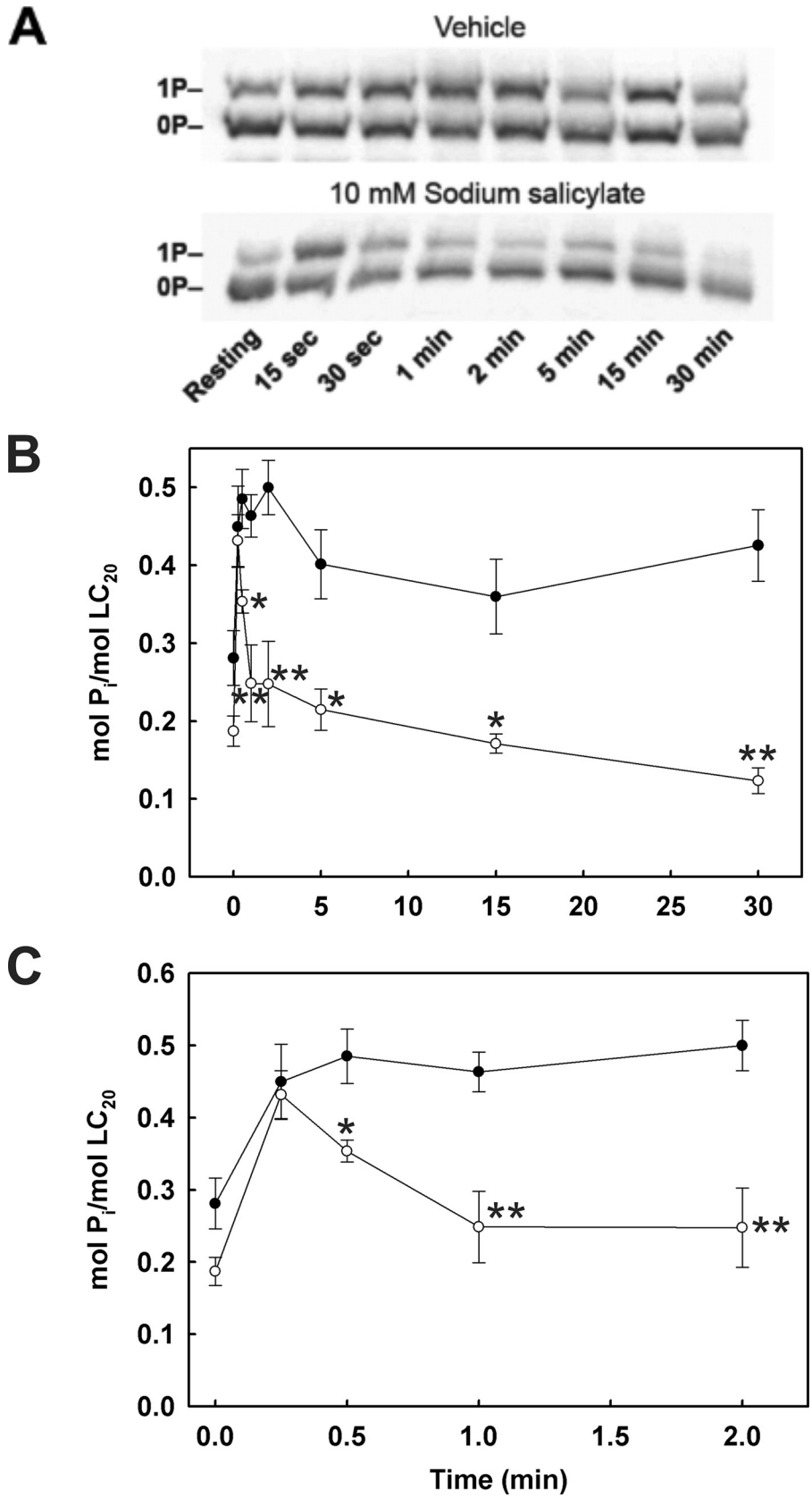


FIGURE 2. **Effect of pre-treatment with sodium salicylate on $K^+$-induced $LC_{20}$ phosphorylation.** Rat caudal arterial smooth muscle strips, pre-incubated with vehicle or sodium salicylate (10 mM), were stimulated at time 0 with $K^+$. *A* and *B*, tissues were quick-frozen at the indicated times for analysis of $LC_{20}$ phosphorylation by Phos-tag SDS-PAGE (*A*), and phosphorylation stoichiometry was determined by densitometric scanning of the unphosphorylated (*0P*) and phosphorylated (*1P*) bands detected by anti-$LC_{20}$ (*B*). Values represent the mean ± S.E. ($n = 4–5$). *, $p < 0.05$ and **, $p < 0.01$, significantly different from the level of $LC_{20}$ phosphorylation in the absence of salicylate. *C*, an expanded version of the first 2 min of the time course depicted in *B*.

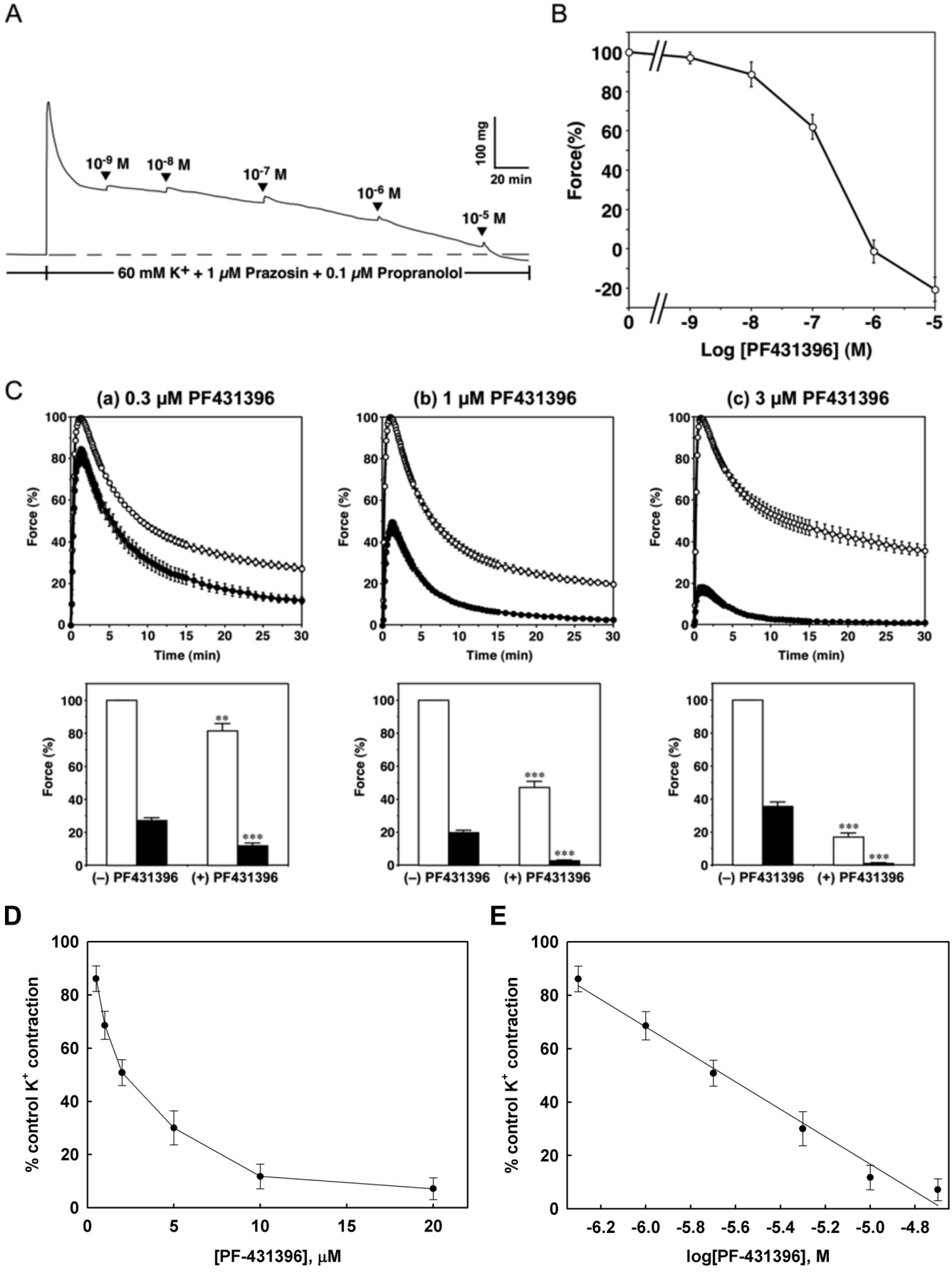
A
10-9 M
10-8 M
10-7 M
10-6 M
10-5 M
100 mg
20 min
60 mM K+ + 1 μM Prazosin + 0.1 μM Propranolol
B
Force(%)
Log [PF431396] (M)
C
(a) 0.3 μM PF431396
(b) 1 μM PF431396
(c) 3 μM PF431396
Force (%)
Time (min)
(–) PF431396
(+) PF431396
D
% control K+ contraction
[PF-431396], μM
E
% control K+ contraction
log[PF-431396], M

**TABLE 1**

**Inhibition of peak and sustained $K^+$-induced contraction by Pyk2/FAK inhibitors**

Rat caudal arterial smooth muscle strips were pre-incubated for 30 min with the indicated inhibitors at various concentrations prior to membrane depolarization. Contractile responses to $K^+$ were recorded and peak and sustained force levels were measured.

| Inhibitor | $IC_{50}$ | | | | References |
|---|---|---|---|---|---|
| | Peak contraction | Sustained contraction | Pyk2 activity[a] | FAK activity[a] | |
| | | $\mu M$ | | | |
| PF-431396 | 2.4 ± 0.16 | 0.49 ± 0.07 | 0.031 | 0.001 | 14 |
| PF-562271 | 2.7 ± 0.52 | 0.80 ± 0.03 | 0.014 | 0.0015 | 15 |
| PF-573228 | 10.0 ± 4.55 | 0.62 ± 0.06 | >1 | 0.004 | 16 |
| NVP-TAE226 | 0.82 ± 0.03 | 0.21 ± 0.07 | 0.002–0.005 | 0.007 | 17, 18 |
| sc-203950 | 41 ± 19 | 44 ± 26 | >1 | 1 | 19 |

[a] $IC_{50}$ values for inhibition of Pyk2 and FAK are taken from the literature with the relevant references provided in the right-hand column.

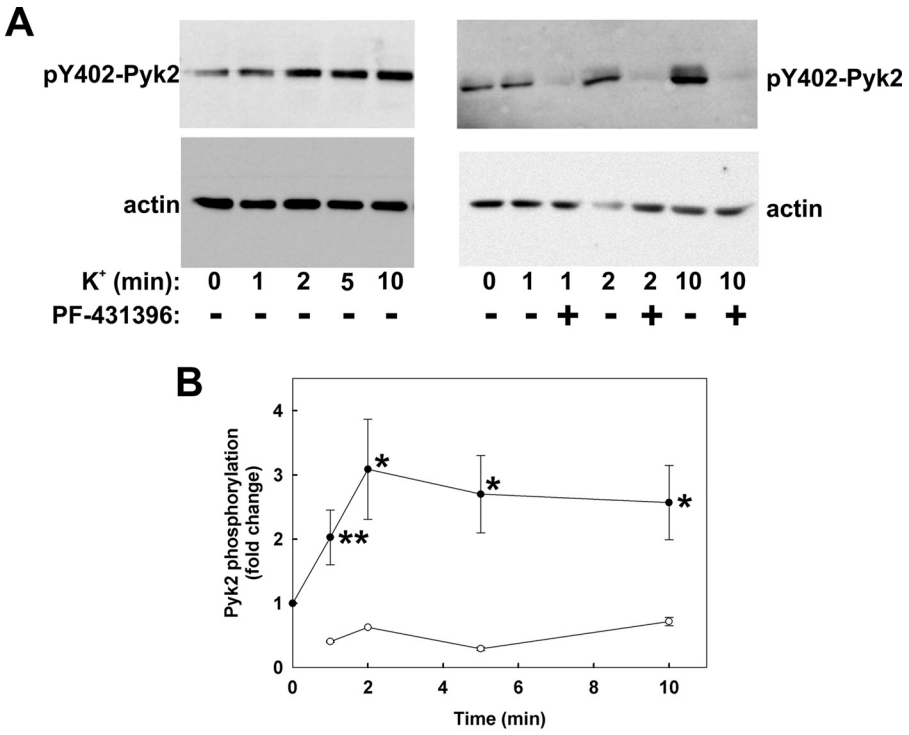


FIGURE 4. **Effect of $K^+$-induced depolarization on Pyk2 autophosphorylation and its sensitivity to PF-431396.** Rat caudal arterial smooth muscle strips were stimulated at time 0 with $K^+$ following pre-incubation for 30 min with vehicle or PF-431396 (10 $\mu$M). Tissues were quick-frozen at the indicated times for analysis of Pyk2 autophosphorylation at Tyr-402 by SDS-PAGE and Western blotting with anti-pTyr-402-Pyk2. Loading levels were normalized to actin. *A*, representative Western blots for phosphorylated Tyr-402 Pyk2 (*pY402-Pyk2*) and actin. *B*, cumulative quantitative data expressed as -fold change relative to untreated tissue and normalized to actin. Values represent the mean ± S.E. ($n = 13$ for *solid circles* and $n = 5$ for *open circles*). *, $p < 0.01$, **, $p < 0.02$, significantly different from Pyk2 phosphorylation level prior to membrane depolarization.

chemiluminescence detection, as described previously (6–8). Interestingly, we found that transfer of Pyk2 to nitrocellulose membranes required SDS in the transfer buffer, whereas transfer of FAK was optimal in the absence of SDS. The levels of phosphorylation of Pyk2 at Tyr-402 and FAK at Tyr-397 were calculated from the ratio of signal intensities for pTyr-402-Pyk2 or pTyr-397-FAK:total Pyk2/FAK and/or actin. Anti-Pyk2 rabbit polyclonal antibody (Sigma, catalogue number SAB4500837) was used at 1:1500 dilution, and anti-pTyr-402-Pyk2 rabbit polyclonal antibody (Invitrogen, catalogue number 44-618G) was used at 1:1500 dilution. Anti-pTyr-397-FAK (Cell Signaling, catalogue number 3283) and anti-FAK (Cell

FIGURE 3. **Effect of PF-431396 on $K^+$-induced contraction.** *A*, representative tracing showing the inhibitory effect of PF-431396 on $K^+$-induced sustained contraction of rat caudal arterial smooth muscle. PF-431396 was added once $K^+$-induced contraction became stable. *B*, concentration dependence of PF-431396-mediated inhibition of $K^+$-induced sustained contraction. Force is expressed as a percentage of the sustained contraction in response to $K^+$ before the addition of the drug. Values represent the mean ± S.E. ($n = 7$). *C*, effect of pre-treatment with PF-431396 on $K^+$-induced contraction of rat caudal arterial smooth muscle. *Upper panels* show the time courses of $K^+$-induced contraction without (○) or with (●) PF-431396 at the indicated concentrations. *Lower panels* show cumulative data on the effects of PF-431396 on the phasic and tonic components of $K^+$-induced contraction. Force is expressed as a percentage of the maximal force of the phasic contraction induced by $K^+$ without PF-431396. *Open bars* indicate the phasic contraction in response to $K^+$, and *filled bars* indicate the tonic contraction (30 min after $K^+$ addition). Values represent the mean ± S.E. ($n = 7$ for the data in the presence of 0.3 or 1 $\mu$M PF-431396; $n = 8$ for the data in the presence of 3 $\mu$M PF-431396). **, $p < 0.01$ and ***, $p < 0.001$, significantly different from the value of the force without PF-431396. *D* and *E*, concentration dependence of the effect of PF-431396 on the phasic contractile response to $K^+$. Rat caudal arterial smooth muscle strips were pre-incubated with PF-431396 at the indicated concentrations for 30 min prior to stimulation with $K^+$ in the continued presence of PF-431396. The maximal contractile responses at each drug concentration are expressed as a percentage of maximal $K^+$-induced contraction in the absence of inhibitor and are plotted as a function of drug concentration (on a linear scale in *D* and on a log scale in *E*). Values represent the mean ± S.E. ($n = 6$).

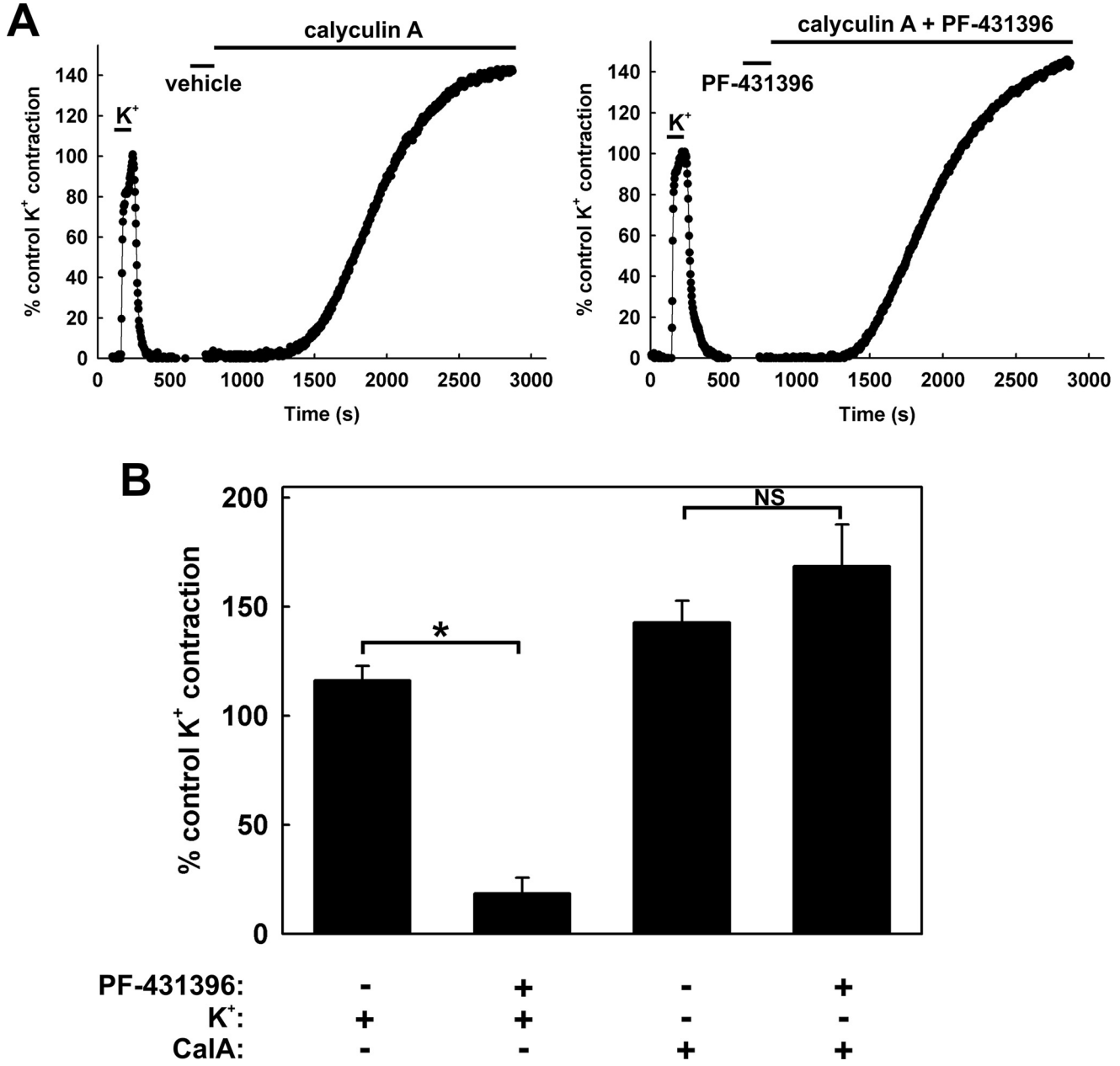


FIGURE 5. **Effect of PF-431396 on calyculin A-induced contraction.** *A*, following a control $K^+$-induced contraction to verify tissue viability, rat caudal arterial smooth muscle strips were pre-incubated with vehicle (*left panel*) or PF-431396 (20 $\mu$M) (*right panel*) for 30 min prior to stimulation with the membrane-permeant protein Ser/Thr phosphatase inhibitor calyculin A (0.5 $\mu$M). *B*, cumulative quantitative data. Values represent the mean ± S.E. ($n = 3$), and force is expressed relative to the control $K^+$-induced contractions. *CalA*, calyculin A. *, $p < 0.001$; *NS*, not significantly different ($p = 0.30$).

Signaling, catalogue number 3285) were used at 1:1000 dilution. The level of phosphorylation of MYPT1 at Thr-697 and Thr-855 was calculated from the ratio of signal intensities for pThr-697-MYPT1 or pThr-855-MYPT1:total MYPT1. Anti-pThr-697-MYPT1 rabbit polyclonal antibody (Millipore, catalogue number ABS45) was used at 1:3500 dilution, anti-pThr-855-MYPT1 rabbit polyclonal antibody (Millipore, catalogue number 36-003) was used at 1:3000 dilution, and anti-MYPT1 rabbit polyclonal antibody (Santa Cruz Biotechnology, catalogue number sc-25618) was used at 1:250 dilution. Anti-pTyr monoclonal antibody, clone 4G10, was purchased from Millipore (catalogue number 05-321), and monoclonal antibody P-Tyr-100 was purchased from Cell Signaling (catalogue number 9411). For phosphotyrosine Western blots, transfer to nitrocellulose membranes was carried out with SDS in the transfer buffer; if SDS was eliminated, there was little transfer of phosphotyrosine-containing proteins. In the case of Phos-tag SDS-PAGE (which separates phosphorylated and unphosphorylated forms of $LC_{20}$), anti-$LC_{20}$ rabbit polyclonal antibody (Santa Cruz Biotechnology, catalogue number sc-15370) was used at 1:500 dilution.

*RhoA Translocation*—Separation of particulate and cytosolic fractions was achieved by the method of Gong *et al.* (9) as described in detail by Mita *et al.* (6).

*ROK Assay*—ROK$\alpha$ (ROCKII) (Millipore; catalogue number 14-338) (0.1 $\mu$g/ml) was incubated at 30 °C in 20 mM Tris-HCl,

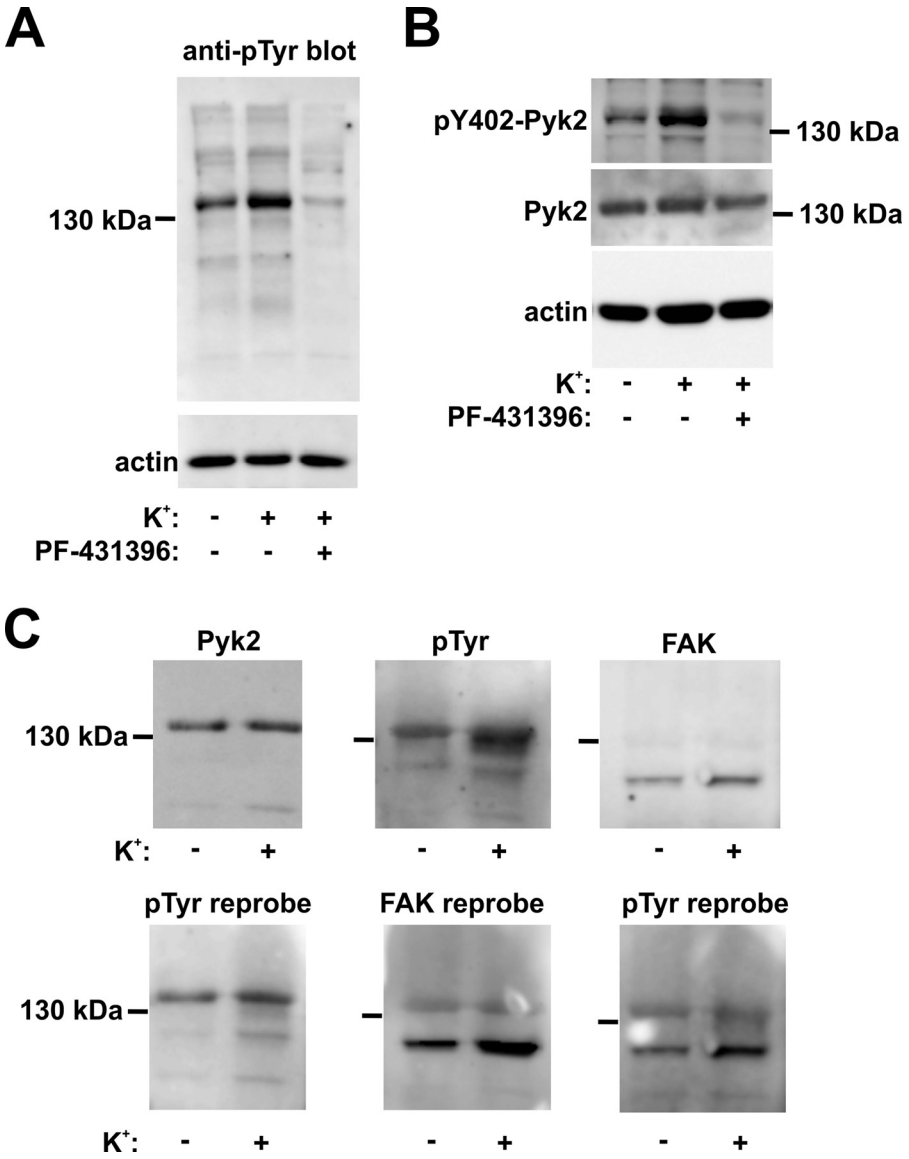


FIGURE 6. **Pyk2 is the major tyrosine-phosphorylated protein in $K^+$-stimulated rat caudal arterial smooth muscle.** Rat caudal arterial smooth muscle strips were pre-incubated with PF-431396 (10 $\mu$M) or vehicle for 30 min prior to stimulation with $K^+$ for 10 min in the absence or presence of inhibitor. *A* and *B*, tissues were quick-frozen for analysis of protein tyrosine phosphorylation (*A*) and Pyk2 autophosphorylation (*B*) by Western blotting with anti-pTyr and anti-pTyr-402-Pyk2 (*pY402-Pyk2*), respectively. Actin was used as the loading control. *C*, control tissues and tissues treated for 10 min with $K^+$ were subjected to SDS-PAGE and Western blotting with antibodies to Pyk2, pTyr, or FAK as indicated in the *upper panel*. The position of the 130-kDa marker is indicated. Blots were reprobed (*lower panel*) with anti-pTyr, anti-FAK, and anti-pTyr, respectively. Blots are representative of ≥3 replicates.

pH 7.5, 5 mM EGTA, 5 mM $MgCl_2$, 1 mM DTT with 0.1 mg/ml MYPT1 peptide (RQSRRSTQGVTLTC) containing Thr-697 (T) in the absence and presence of sodium salicylate (3 or 10 mM). Reactions were started by the addition of 2 mM [$\gamma$-$^{32}$P]ATP (~500 cpm/pol). Samples (20 $\mu$l) of reaction mixtures were withdrawn after 0.5, 1, 1.5, 2, 2.5, and 3 min for quantification of $^{32}$P incorporation as described previously (10). Reactions were linear over this time course. The MYPT1 peptide was synthesized in the Peptide Synthesis Core Facility at the University of Calgary. The purity of the peptide (>95%) was confirmed by analytical high-performance liquid chromatography and amino acid analysis.

*Statistical Analysis*—Data represent the mean ± S.E. Values of *n* indicate the numbers of muscle strips utilized. Student's *t* test was used for statistical comparisons. One-way analysis of variance followed by Tukey-Kramer multiple-comparisons test was used to compare three or more groups. $p$ values $<$ 0.05 were considered to be statistically significant. These analyses were performed using JMP-5J (SAS Institute) or SigmaPlot.

## RESULTS

Sodium salicylate has been identified as an inhibitor of Pyk2 (11), and its unique ability among non-steroidal anti-inflammatory drugs to induce vasodilation has been attributed to this action rather than its cyclooxygenase inhibitory activity (12). Incremental addition of sodium salicylate after steady-state force was attained in response to $K^+$-induced membrane depolarization of rat caudal arterial smooth muscle strips, and resulted in concentration-dependent relaxation with an $IC_{50}$ of

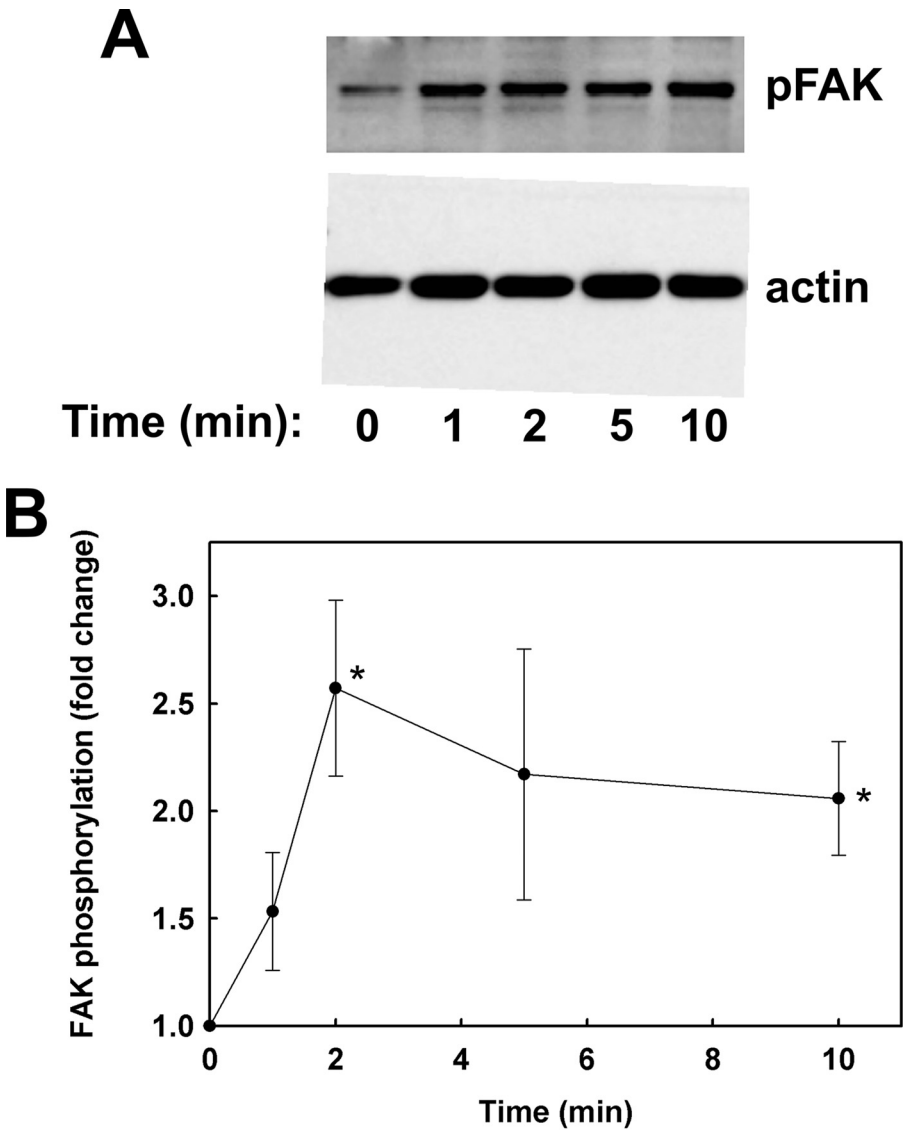


FIGURE 7. **Effect of $K^+$-induced depolarization on FAK autophosphorylation.** Rat caudal arterial smooth muscle strips were stimulated at time 0 with $K^+$. Tissues were quick-frozen at the indicated times for analysis of FAK autophosphorylation at Tyr-397 by SDS-PAGE and Western blotting with anti-pTyr-397-FAK. Loading levels were normalized to actin. *A*, representative Western blots for phosphorylated FAK (*pFAK*) and actin. *B*, cumulative quantitative data expressed as -fold change relative to untreated tissue and normalized to actin. Values represent the mean ± S.E. ($n = 8$). *, $p < 0.005$, significantly different from FAK phosphorylation level prior to membrane depolarization.

2.9 ± 0.5 mM ($n = 13$). Furthermore, pre-treatment with sodium salicylate (3 and 10 mM) reduced the tonic component of $K^+$-induced contraction without affecting the phasic component (Fig. 1). This inhibitory effect of sodium salicylate was very similar to that evoked by the ROK inhibitor Y-27632 (3), suggesting that Pyk2 is involved in activation of the RhoA/ROK pathway responsible for force maintenance, but not the phasic contractile response to $Ca^{2+}$ entry leading to MLCK activation. In support of this conclusion, sodium salicylate had no effect on the rapid increase in $LC_{20}$ phosphorylation elicited by membrane depolarization, but abolished the maintenance of $LC_{20}$ phosphorylation levels at longer times corresponding to the sustained phase of the contractile response to $K^+$ (Fig. 2).

The involvement of Pyk2 in the $K^+$-induced contractile response was supported by the inhibitory effect of PF-431396, a Pyk2/FAK inhibitor (13). Following sustained $K^+$-induced contraction, PF-431396 induced a concentration-dependent relaxation with an $IC_{50}$ of 0.3 ± 0.1 μM (Fig. 3, *A* and *B*). Pre-treatment with PF-431396 not only inhibited the tonic component of the $K^+$-induced contractile response ($IC_{50} = 0.49 \pm 0.07$ μM) but also the phasic contraction (Fig. 3*C*) with an $IC_{50}$ of 2.4 ± 0.16 μM (Fig. 3, *D* and E, and Table 1) (14–19).

To determine whether membrane depolarization evokes Pyk2 activation, we investigated the effect of $K^+$ stimulation on the autophosphorylation of Pyk2 at Tyr-402. $K^+$ induced a time-dependent increase in phosphorylation of Pyk2 at Tyr-402 (Fig. 4*A*, *left panel*, and Fig. 4*B*). The time course of Pyk2 activation is consistent with its involvement in the tonic component of the contractile response to membrane depolarization (compare Figs. 1 and 4). The $t_{½}$ of the phasic $K^+$-induced contraction was 12.1 ± 0.5 s, and the time to maximal force was 46.0 ± 2.0 s ($n = 76$). PF-431396 pre-treatment inhibited basal (see below, Fig. 11*B*) and $K^+$-induced Pyk2 autophosphoryla-

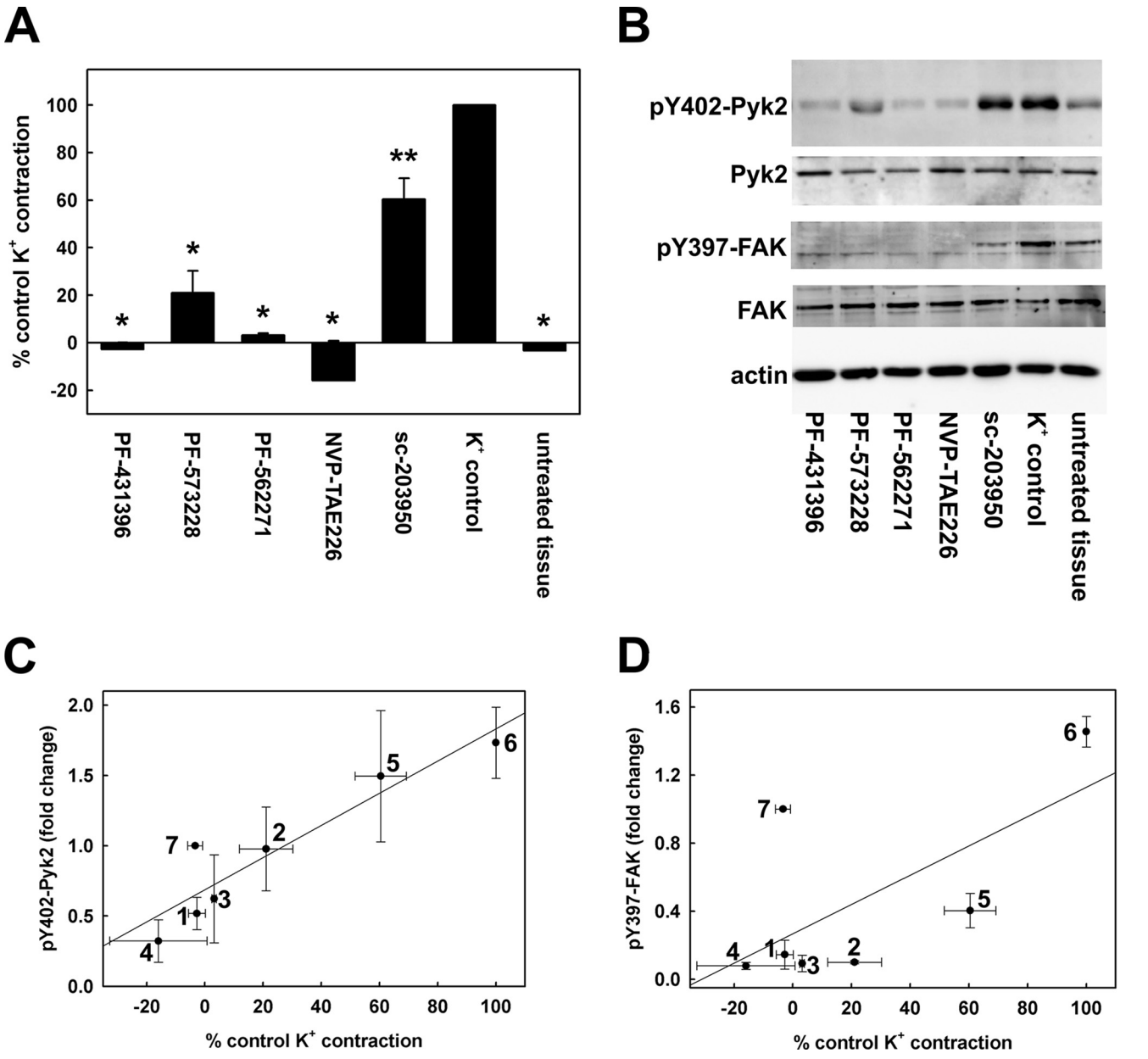


FIGURE 8. **The relationship between inhibition of Pyk2 autophosphorylation and $K^+$-stimulated contraction for various Pyk2/FAK inhibitors.** Rat caudal arterial smooth muscle strips were pre-incubated for 30 min with PF-431396, PF-573228, PF-562271, NVP-TAE226, or sc-203950 (2 or 10 $\mu$M) or vehicle and then stimulated with $K^+$ in the continued presence of inhibitor. *A*, force was recorded continuously, and values at 10 min after $K^+$ addition are expressed relative to control $K^+$-induced contractions. Values represent the mean ± S.E. ($n = 6$). *, $p < 0.001$, **, $p < 0.002$, significantly different from the control $K^+$-induced sustained contractile response. *B*, tissues were quick-frozen 10 min after the addition of $K^+$ for analysis of Pyk2 autophosphorylation by Western blotting with anti-pTyr-402-Pyk2 (*pY402-Pyk2*) and FAK autophosphorylation with anti-pTyr-397-FAK (*pY397-FAK*). Actin was used as the loading control, and anti-Pyk2 and anti-FAK were used to verify the total levels of the two proteins. *C* and *D*, relationship between Pyk2 (*C*) and FAK (*D*) autophosphorylation and the magnitude of the tonic $K^+$-induced contractile response. Values represent the mean ± S.E. ($n = 4$ (*C*) and $n = 3$ (*D*)).

tion at Tyr-402 (Fig. 4*A*, *right panel*, and Fig. 4*B*). Although PF-431396 inhibited $K^+$-induced contraction, it had no effect on the contractile response to the membrane-permeant phosphatase inhibitor calyculin-A (Fig. 5), indicating that the Pyk2/FAK inhibitor does not exert an off-target effect downstream of $LC_{20}$ phosphorylation, *e.g.* at the level of cross-bridge cycling.

Pyk2 co-migrates on SDS-PAGE with the major tyrosine-phosphorylated protein in response to $K^+$ treatment (Fig. 6). PF-431396 pre-treatment blocked tyrosine phosphorylation of this band (Fig. 6*A*) and, as shown earlier, abolished the autophosphorylation of Pyk2 at Tyr-402 (Fig. 6*B*). However, PF-431396 also inhibits the related tyrosine kinase FAK (13), and we observed that FAK autophosphorylation at Tyr-397 (equivalent to Tyr-402 of Pyk2) is increased upon $K^+$ stimulation of rat caudal arterial smooth muscle in a time-dependent manner (Fig. 7). We were able to separate Pyk2 and FAK on 7.5% acrylamide SDS gels, and the results showed that Pyk2, but not FAK, co-migrated with the major tyrosine-phosphorylated band (Fig. 6*C*, *upper blots*). Reprobing these anti-Pyk2, -pTyr, and -FAK blots with anti-pTyr, -FAK, and -pTyr, respectively, clearly indicated that Pyk2 and not FAK is the major tyrosine-

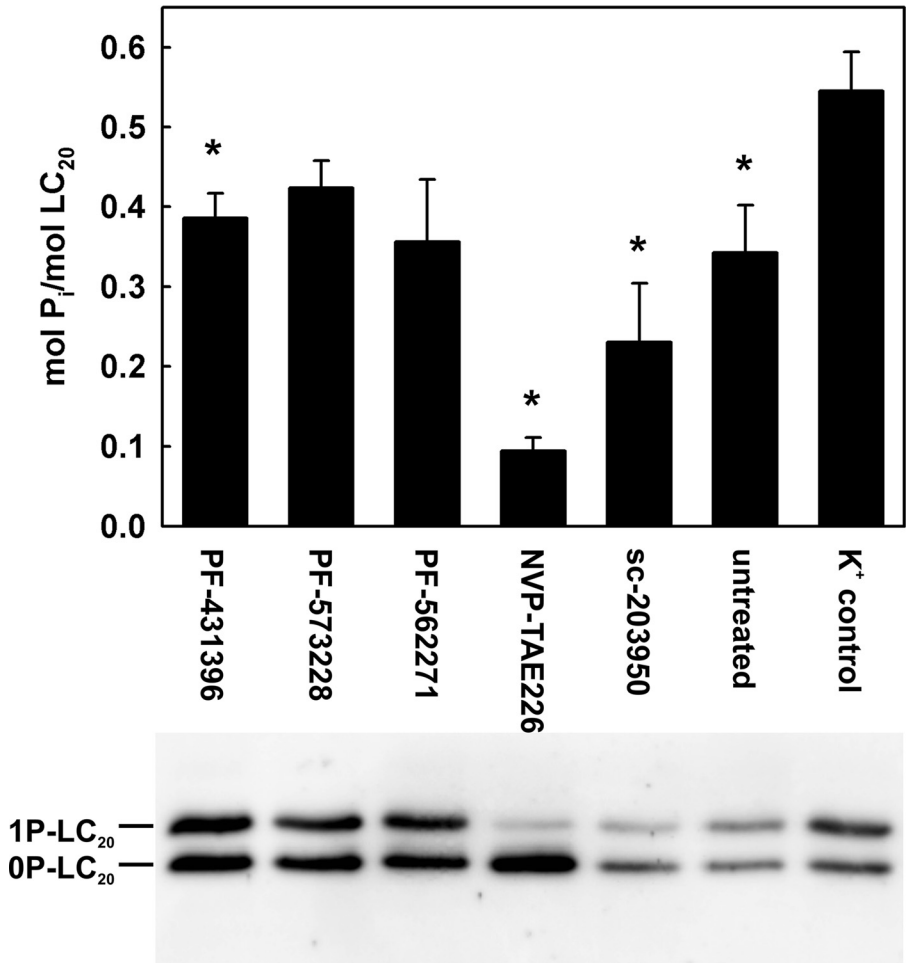


FIGURE 9. **Effect of Pyk2/FAK inhibitors on $K^+$-induced $LC_{20}$ phosphorylation.** Rat caudal arterial smooth muscle strips were pre-incubated for 30 min with the indicated inhibitors (10 $\mu$M) and then treated with $K^+$ for 10 min in the continued presence of inhibitor. Control strips were pre-incubated in Hepes-Tyrode's solution without inhibitor and either induced to contract with $K^+$ (*$K^+$ control*) or left in Hepes-Tyrode's solution (*untreated*). Phosphorylated (*1P-$LC_{20}$*) and unphosphorylated (*0P-$LC_{20}$*) forms of $LC_{20}$ were separated by Phos-tag SDS-PAGE and detected by Western blotting with anti-$LC_{20}$, and phosphorylation stoichiometry was quantified by scanning densitometry. Values represent the mean ± S.E. ($n = 5$). *, $p < 0.04$, significantly different from the level of $LC_{20}$ phosphorylation in the $K^+$ control. *p* values were as follows (compared with $K^+$ control): PF-431396, 0.024; PF-573228, 0.074; PF-562271, 0.096; NVP-TAE226, 0.00003; sc-203950, 0.012; untreated, 0.039.

phosphorylated protein in $K^+$-stimulated tissue (Fig. 6*C*, *lower blots*).

To distinguish functionally between Pyk2 and FAK, the effects on $K^+$-induced contraction (Fig. 8*A*) and Pyk2 activation (Fig. 8*B*) of several inhibitors with similar and different inhibitory potencies toward these tyrosine kinases were examined. A close correlation ($r^2 = 0.87$) was found between the ability of these inhibitors to inhibit Pyk2 autophosphorylation and $K^+$-induced contraction (Fig. 8*C* and Table 1). This was not the case for FAK, however ($r^2 = 0.44$) (Fig. 8*D* and Table 1), suggesting that Pyk2 rather than FAK plays an important role in the contractile response to membrane depolarization. The Pyk2/FAK inhibitors also affected sustained $K^+$-induced $LC_{20}$ phosphorylation with relative potencies that matched their effects on Pyk2 rather than FAK (Fig. 9 and Table 1).

Sodium orthovanadate, a tyrosine phosphatase inhibitor, has long been known to induce vascular smooth muscle contraction (20). We investigated the possibility that vanadate may act by unmasking the basal activity of Pyk2. In support of this hypothesis, vanadate evoked a slow, sustained contraction (Fig. 10*A*, *left panel*) that was abolished by pre-incubation with PF-431396 (Fig. 10*A*, *right panel*) with an $IC_{50}$ of 66 ± 17 nM (Fig. 10, *C* and *D*). Pyk2 autophosphorylation increased with a similar time course to contraction (Fig. 10*B*, *left panel*), and vanadate-induced Pyk2 autophosphorylation was abolished by pre-treatment with PF-431396 (Fig. 10*B*, *right panel*).

To determine whether Pyk2 activation is indeed downstream of $Ca^{2+}$ influx, the $Ca^{2+}$ ionophore ionomycin was used to increase $[Ca^{2+}]_i$, and Pyk2 activation was assessed by measurements of Tyr-402 phosphorylation. In the presence of extracellular $Ca^{2+}$, ionomycin induced a slow, sustained contraction (Fig. 11*A*, *left panel*) that was inhibited by pre-incubation with PF-431396 (Fig. 11*A*, *right panel*) with an $IC_{50}$ of 2.6 ± 0.7 $\mu$M ($n = 4$). Ionomycin induced an increase in Pyk2 autophosphorylation in a $Ca^{2+}$-dependent manner, and this was also inhibited by pre-treatment with the Pyk2 inhibitor (Fig. 11, *C* and *D*). We also examined the effect of blockade of voltage-gated $Ca^{2+}$ channels by nifedipine on $K^+$-induced contraction and Pyk2 autophosphorylation. Nifedipine inhibited peak (Fig. 12*A*) and sustained $K^+$-induced force (Fig. 12*B*), as well as Pyk2 phosphorylation at Tyr-402 (Fig. 12, *C* and *D*), in a concentration-dependent manner. We conclude from these ionomycin and nifedip-

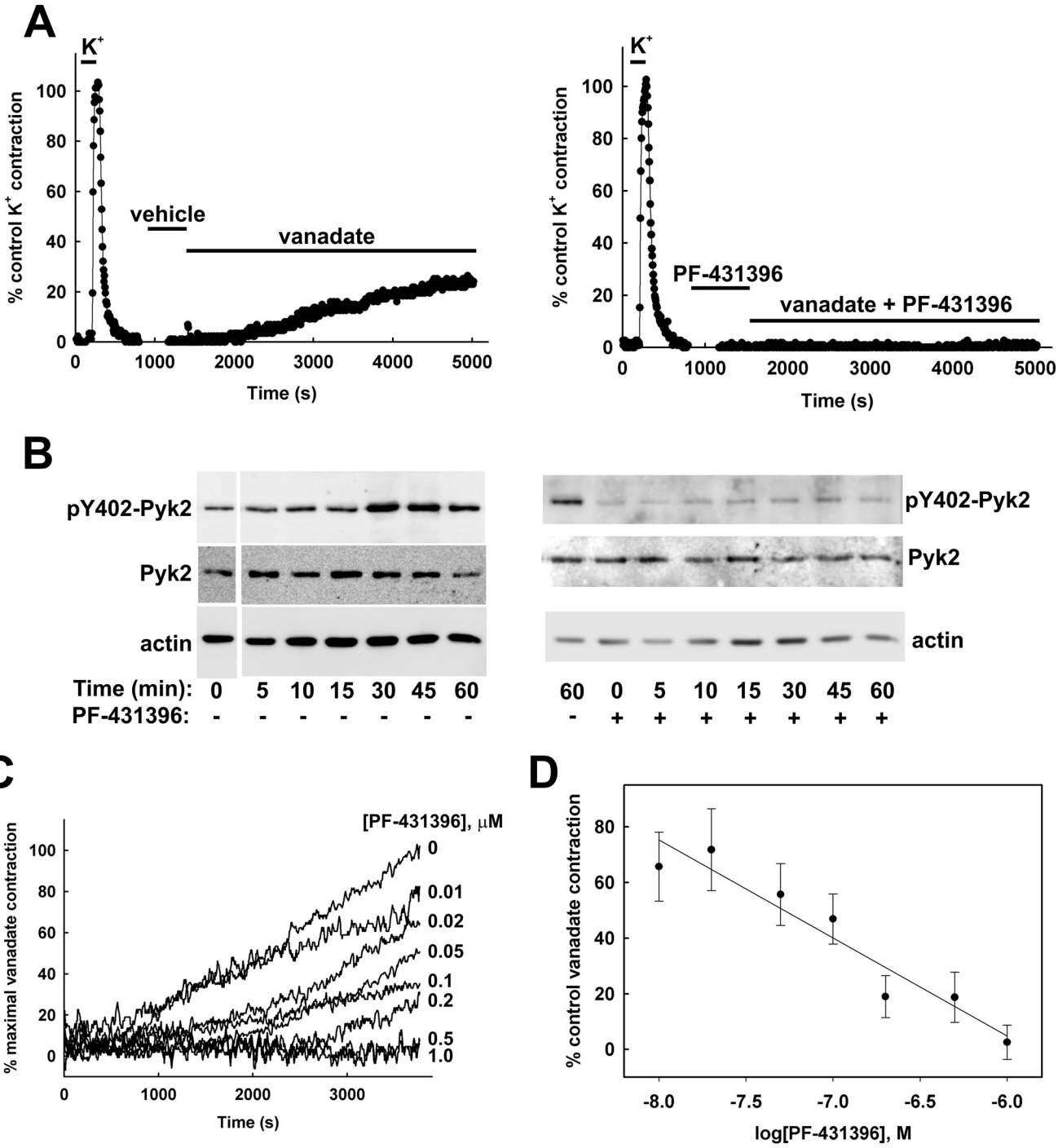


FIGURE 10. **Effect of vanadate on contraction and Pyk2 autophosphorylation, and sensitivity to PF-431396.** *A*, following a control $K^+$-induced contraction to verify tissue viability, rat caudal arterial smooth muscle strips were pre-incubated for 30 min with vehicle (*left panel*) or PF-431396 (20 μM) (*right panel*) and then treated with sodium orthovanadate (5 mM). Force was recorded continuously, and results are representative of three independent experiments. *B*, tissues were quick-frozen at the indicated times of vanadate treatment for analysis of Pyk2 autophosphorylation at Tyr-402 (*pY402-Pyk2*) by Western blotting. Actin was used as loading control, and Pyk2 content was also analyzed. Blots are representative of 4 replicates (*left panel*) and 2 replicates with 5 additional replicates of the 30-min vanadate-treated tissue in the absence and presence of PF-431396 (*right panel*). *C*, the concentration-dependent effect of PF-431396 on vanadate-induced contraction. Tissues were incubated for 30 min with the indicated concentrations of PF-431396 prior to the addition of vanadate (5 mM) at time 0. *D*, cumulative data showing the concentration dependence of inhibition of vanadate-induced contraction by PF-431396. Force was measured 60 min after the addition of vanadate and expressed as a percentage of maximal vanadate-induced contraction. Values indicate mean ± S.E. ($n = 6$).

ine experiments that the influx of extracellular $Ca^{2+}$ is responsible for the activation of Pyk2. The MLCK inhibitor ML-9 inhibited $K^+$-induced contraction (Fig. 13, *A* and *B*) and $LC_{20}$ phosphorylation (data not shown) without affecting the $K^+$-induced increase in Pyk2 autophosphorylation (Fig. 13*C*), confirming that Pyk2 lies upstream of MLCK.

A connection from Pyk2 activation to RhoA activation and $Ca^{2+}$ sensitization was made with the observation that pre-

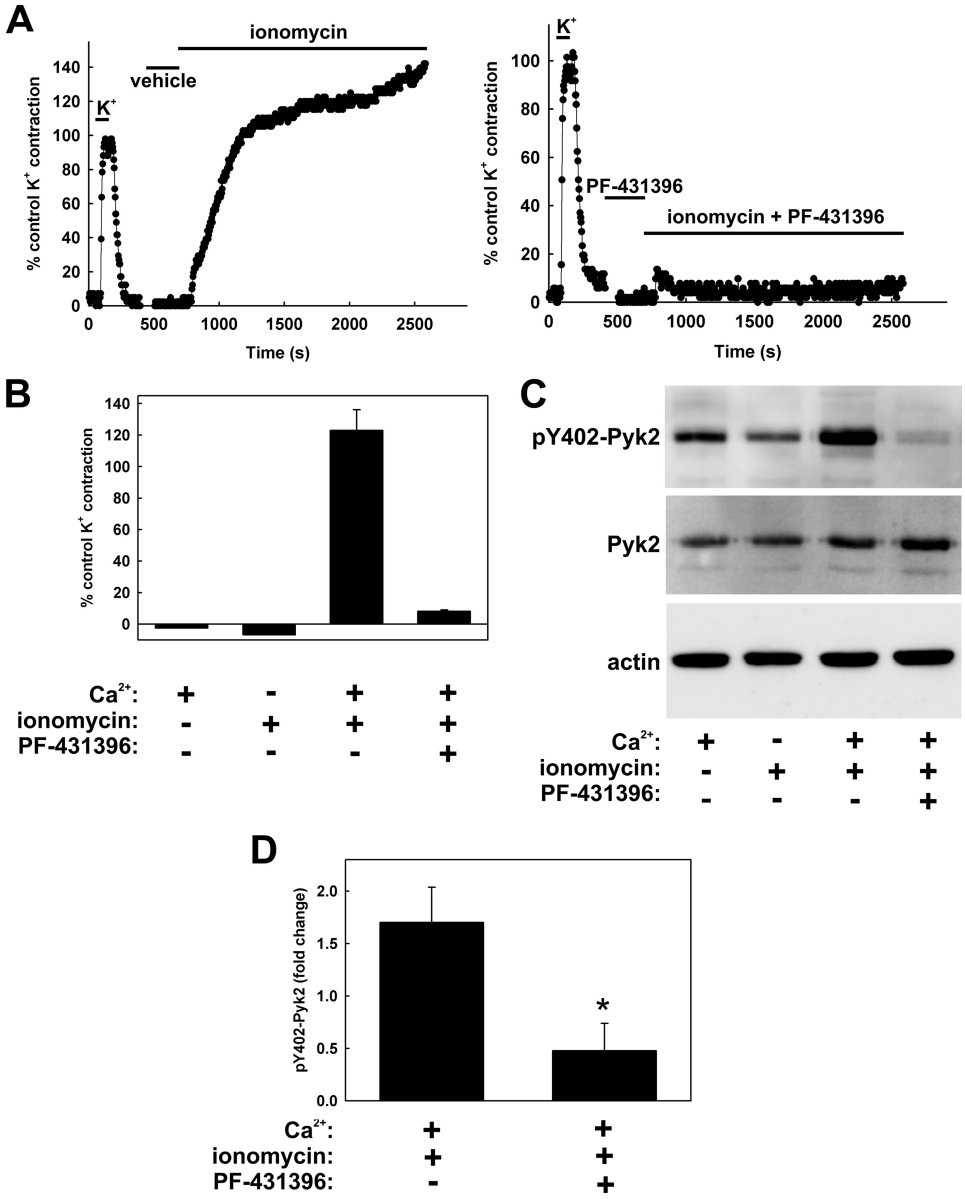


FIGURE 11. **Effect of ionomycin on contraction and Pyk2 autophosphorylation, and sensitivity to PF-431396.** *A*, following a control $K^+$-induced contraction to verify tissue viability, rat caudal arterial smooth muscle strips were pre-incubated for 30 min with vehicle (*left panel*) or PF-431396 (20 $\mu$M) (*right panel*) and then treated with ionomycin (10 $\mu$M) in the presence of extracellular $Ca^{2+}$ (1.8 mM). *B*, cumulative data showing force after a 30-min incubation under the indicated conditions expressed as a percentage of the control $K^+$-induced force ($n = 5$). *C*, tissues were quick-frozen after 30 min of ionomycin (or vehicle) treatment for SDS-PAGE and Western blotting. Representative Western blots show Tyr-402 Pyk2 autophosphorylation (*pY402-Pyk2*), with Pyk2 and actin as loading controls. *D*, cumulative quantitative data expressed as -fold change relative to untreated tissue and normalized to actin to show the effect of PF-431396 on ionomycin-induced Pyk2 autophosphorylation. Values represent the mean ± S.E. ($n = 5$). *, $p <$ 0.05, significantly different from the value in the absence of PF-431396.

treatment with sodium salicylate prevented (i) the $K^+$-induced translocation of RhoA from the cytosol to the membrane (Fig. 14) and (ii) the increase in phosphorylation of MYPT1 at Thr-855 and Thr-697 (Fig. 15). Finally, it was important to demonstrate that sodium salicylate does not have an off-target effect on ROK. An *in vitro* kinase assay indicated that purified ROK was unaffected by sodium salicylate; the rates of phosphorylation of MYPT1 peptide by ROK were 70.5 ± 1.9 $\mu$mol $P_i$/min/mg of ROK in the absence of sodium salicylate, 66.5 ± 2.9 $\mu$mol $P_i$/min/mg of ROK in the presence of 3 mM sodium salicylate, and 65.4 ± 3.4 $\mu$mol $P_i$/min/mg of ROK in the presence of 10 mM sodium salicylate (values indicate the mean ± S.E., $n = 3$ in each case).

## DISCUSSION

Pyk2 (also known as FAK2, CAK$\beta$, and RAFTK) is a non-receptor, $Ca^{2+}$-dependent protein-tyrosine kinase (21). Activation of Pyk2 involves autophosphorylation at Tyr-402, which enables the binding of Src via its SH2 domain and phosphorylation at Tyr-579 and Tyr-580 of Pyk2 within the kinase domain activation loop to generate maximal kinase activity. Kohno *et al.* (22) have proposed that the FERM domain of Pyk2 regu-

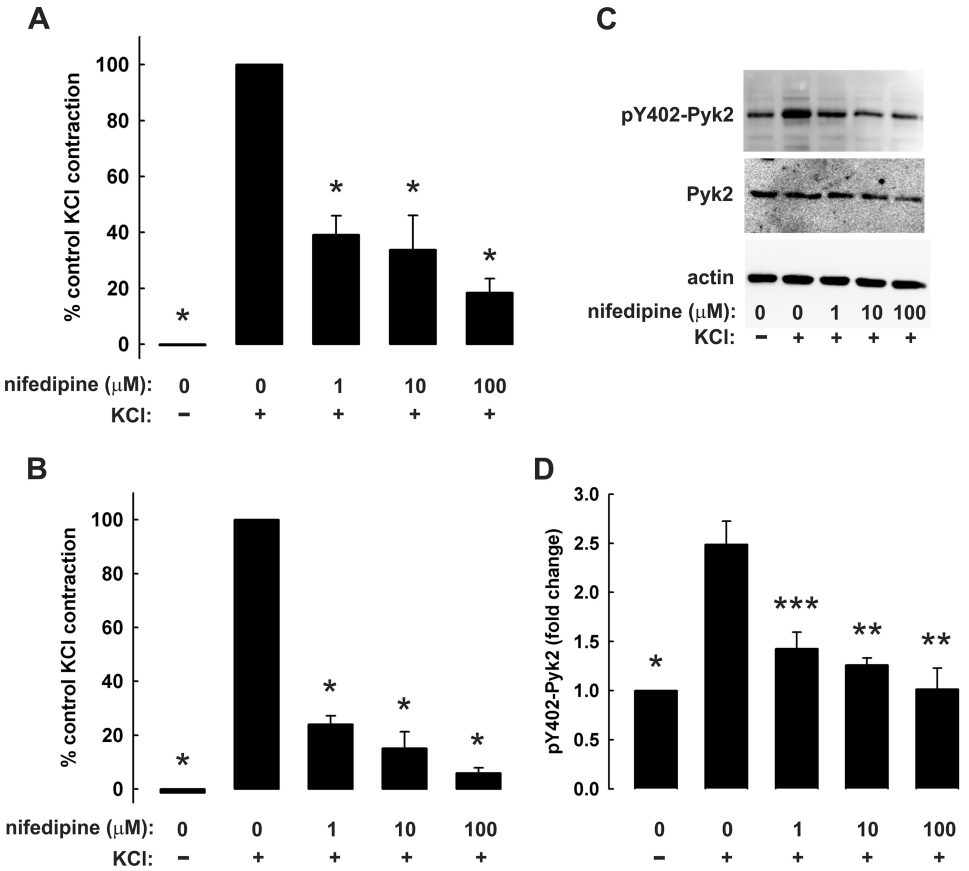


FIGURE 12. **Effects of nifedipine on $K^+$-induced contraction and Pyk2 autophosphorylation.** *A* and *B*, peak (*A*) and sustained (*B*) contractile responses to $K^+$ were recorded in the absence and presence of the indicated concentrations of nifedipine after a 30-min pre-incubation with nifedipine or vehicle (Hepes-Tyrode's buffer). Peak force was recorded 1 min after the addition of $K^+$ and sustained force at 10 min, and values are expressed as a percentage of the peak (*A*) or sustained (*B*) force in tissues treated with $K^+$ in the absence of $Ca^{2+}$ channel blocker ($n = 4–5$). Tissues were quick-frozen after a 10-min treatment with $K^+$ for analysis of Pyk2 autophosphorylation by Western blotting. *C*, representative Western blots showing Pyk2 phosphorylation at Tyr-402 (*pY402-Pyk2*), total Pyk2, and actin as loading control. *D*, cumulative quantitative data with Pyk2 autophosphorylation expressed as -fold change relative to untreated tissue. Values represent the mean ± S.E. ($n = 5$). *, $p < 0.001$, **, $p < 0.05$, ***, $p < 0.01$, significantly different from the value of the $K^+$-treated control in the absence of nifedipine.

lates its activity by mediating $Ca^{2+}$/calmodulin-dependent Pyk2 homodimer formation and transphosphorylation.

Our previous studies indicated that depolarization-induced $Ca^{2+}$ entry elicits $Ca^{2+}$ sensitization of vascular smooth muscle contraction via activation of the RhoA/ROK pathway (3) and implicated a genistein-sensitive tyrosine kinase upstream of RhoA activation (6). We considered Pyk2 as a strong candidate given its $Ca^{2+}$ dependence. This possibility was supported by the observation that sodium salicylate (a known inhibitor of Pyk2) relaxed rat caudal arterial smooth muscle pre-contracted by membrane depolarization and that the tonic, but not the phasic component of $K^+$-induced contraction was abolished by pre-treatment with salicylate (Fig. 1). This effect of salicylate was very similar to that of the ROK inhibitor Y-27632 (3). Consistent with these effects on force, sodium salicylate pre-treatment had no effect on the rapid increase in $LC_{20}$ phosphorylation induced by membrane depolarization, but abolished the sustained elevation of $LC_{20}$ phosphorylation (Fig. 2). The Pyk2/FAK inhibitor PF-431396, on the other hand, inhibited both phasic and tonic components of $K^+$-induced force (Fig. 3) and $LC_{20}$ phosphorylation (Fig. 9), suggesting an off-target effect of this compound during the phasic contraction. A likely target is MLCK itself because skeletal muscle MLCK has been shown to be partially inhibited by PF-431396 (13).

One of the most important findings of this study was that Pyk2 autophosphorylation at Tyr-402, which correlates with activation of the enzyme (21), increased in response to membrane depolarization (Fig. 4) with a time course corresponding to that of the tonic component of the contractile response (Fig. 1). Furthermore, Pyk2 was identified as the major tyrosine-phosphorylated protein in response to membrane depolarization (Fig. 6). As expected, PF-431396 inhibited both basal (Fig. 10*B*) and $K^+$-induced Pyk2 autophosphorylation (Fig. 4). Importantly, PF-431396 had no effect on contraction induced by the membrane-permeant Ser/Thr phosphatase inhibitor calyculin A (Fig. 5). Calyculin A induces a slow, sustained contraction of vascular smooth muscle through inhibition of MLCP, which unmasks the basal activities of integrin-linked kinase and zipper-interacting protein kinase, leading to phosphorylation of $LC_{20}$ at Thr-18 and Ser-19 and contraction (7). The fact that PF-431396 had no effect on calyculin A-induced contraction indicates the absence of an off-target effect of the compound downstream of $LC_{20}$ phosphorylation.

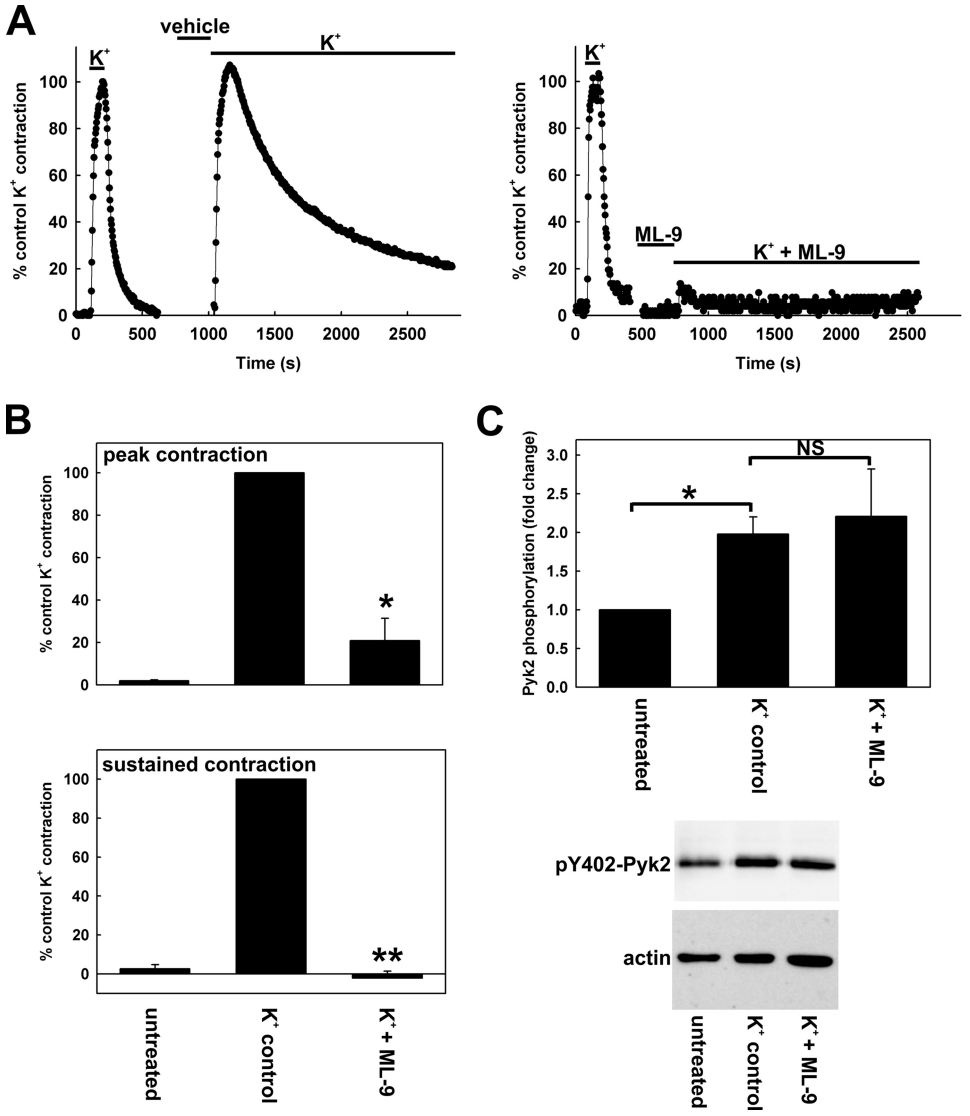


FIGURE 13. **Effects of myosin light chain kinase inhibition on $K^+$-induced contraction and Pyk2 autophosphorylation.** *A* and *B*, representative $K^+$-induced contractions (*A*) and cumulative quantitative data (*B*) showing the effect of pre-incubation with the MLCK inhibitor ML-9 (25 $\mu$M) on peak and sustained (30-min) force. Values represent the mean ± S.E. ($n = 3$). *, $p < 0.01$; **, $p < 0.02$, significantly different from the force in the absence of ML-9. *C*, tissues were quick-frozen 30 min after the addition of $K^+$ for SDS-PAGE and Western blotting with anti-pTyr-402-Pyk2 (*pY402-Pyk2*), with actin as loading control. Representative blots are shown below the cumulative quantitative data. Values represent the mean ± S.E. ($n = 3$). *, $p < 0.02$; *NS*, not significantly different ($p > 0.7$).

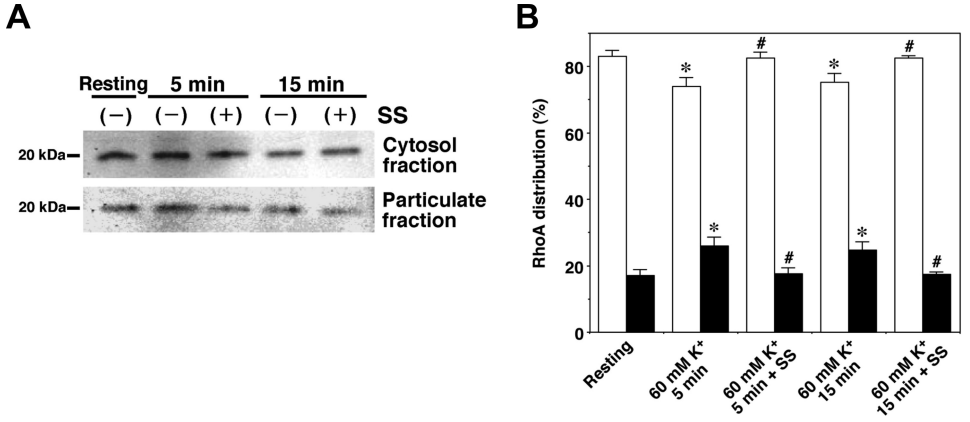


FIGURE 14. **Effect of sodium salicylate on $K^+$-induced translocation of RhoA.** Muscle strips were pre-incubated for 20 min with vehicle or sodium salicylate (*SS*, 3 mM) prior to stimulation with $K^+$ in the absence or presence of salicylate. *A*, representative Western blots showing the $K^+$-induced translocation of RhoA from the cytosolic to the particulate fraction in the absence and presence of salicylate. *B*, cumulative data for the cytosolic (*open bars*) and particulate (*filled bars*) fractions in the absence or presence of sodium salicylate. Values represent the mean ± S.E. ($n = 6–7$). *, $p < 0.05$, significantly different from the value under resting conditions without sodium salicylate; #, $p < 0.05$, significantly different from the value following $K^+$ stimulation for 5 or 15 min.

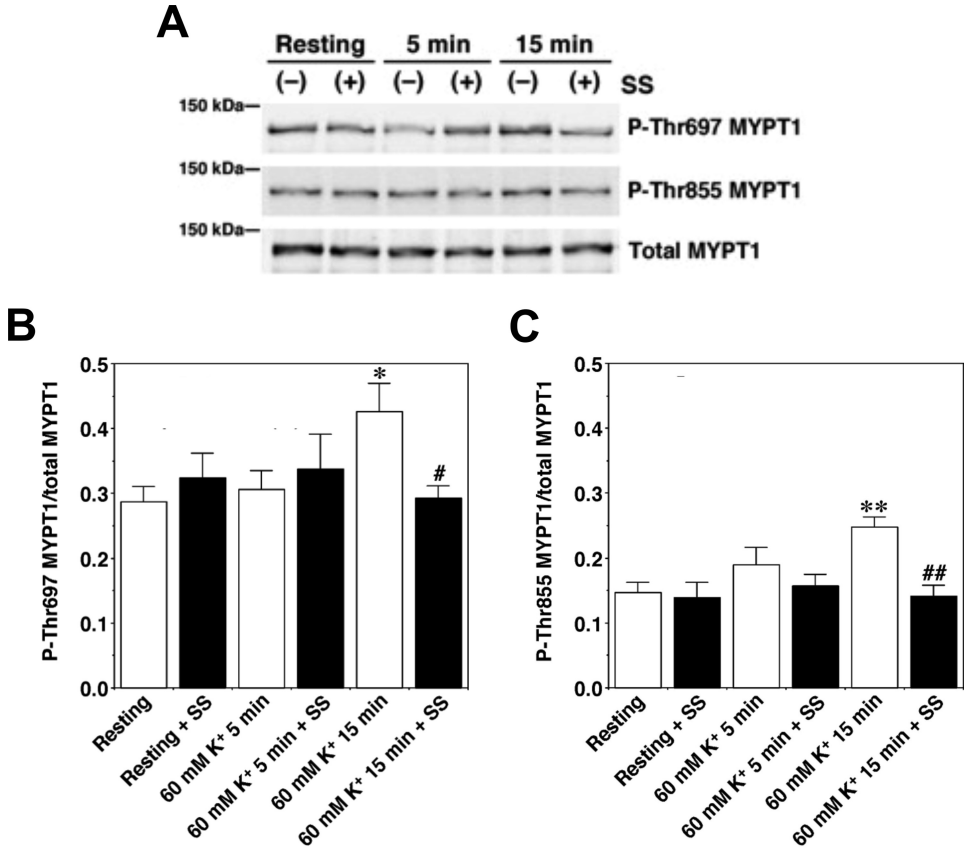


FIGURE 15. **Effects of sodium salicylate on $K^+$-induced phosphorylation of MYPT1 at Thr-697 and Thr-855.** *A*, representative Western blots showing $K^+$-induced phosphorylation of MYPT1 at Thr-697 and Thr-855 in the absence or presence of sodium salicylate (*SS*; 3 mM). *B* and *C*, cumulative data of the phosphorylation of MYPT1 at Thr-697 (*B*) and Thr-855 (*C*) in the absence (*open bars*) or presence (*closed bars*) of sodium salicylate (3 mM). Values represent the mean ± S.E. ($n = 5–6$ for pThr-697 and $n = 5$ for pThr-855). *, $p < 0.05$ and **, $p < 0.005$, significantly different from the value under resting conditions without sodium salicylate; #, $p < 0.05$ and ##, $p < 0.005$, significantly different from the value following $K^+$ stimulation for 5 or 15 min in the absence of sodium salicylate.

The related tyrosine kinase FAK was also found to be autophosphorylated at Tyr-397 (which corresponds to Tyr-402 of Pyk2) in response to $K^+$ stimulation, with a time course similar to that of Pyk2 autophosphorylation (Fig. 7). However, quantitatively, Pyk2 tyrosine phosphorylation was found to be considerably greater than that of FAK (Fig. 6), and the relationship between autophosphorylation and contraction in the presence of various Pyk2/FAK inhibitors was linear for Pyk2 (Fig. 8*C*; $r^2 = 0.87$) but not for FAK (Fig. 8*D*; $r^2 = 0.44$). We conclude, therefore, that Pyk2 plays a major role in sustained $K^+$-induced contraction.

Use of the tyrosine phosphatase inhibitor sodium orthovanadate further supported a role for Pyk2 in sustained contraction of vascular smooth muscle. Thus the slow, sustained contraction induced by vanadate was abolished by pre-treatment with PF-431396, and this correlated with attenuation of vanadate-induced Pyk2 autophosphorylation (Fig. 10).

Treatment of rat caudal arterial smooth muscle strips with the $Ca^{2+}$ ionophore ionomycin induced Pyk2 autophosphorylation at Tyr-402 and a slow, sustained contractile response, both of which were blocked by pre-incubation with PF-431396 (Fig. 11), indicating that $Ca^{2+}$ influx activates Pyk2 and contraction. The $IC_{50}$ for inhibition of ionomycin-induced contraction was determined to be 2.6 ± 0.7 μM, *i.e.* similar to the $IC_{50}$ (2.4 ± 0.16 μM) for PF-431396-mediated inhibition of the phasic component of the $K^+$-induced contraction (see above). These observations are consistent with (i) a slow ionomycin-induced increase in $[Ca^{2+}]_i$ leading to slow activation of MLCK and sustained contraction due to the maintenance of elevated $[Ca^{2+}]_i$ and (ii) activation of Pyk2 by $Ca^{2+}$, which is not required for ionomycin-induced contraction. That is, Pyk2-mediated inhibition of MLCP is not required for the sustained ionomycin-induced contraction because the increase in $[Ca^{2+}]_i$ is presumably sufficient to activate MLCK to a level that overcomes that of MLCP. The conclusion that $Ca^{2+}$ entry is responsible for Pyk2 activation was supported by the observation that the $Ca^{2+}$ channel blocker nifedipine inhibited both $K^+$-induced force and Pyk2 autophosphorylation (Fig. 12).

Finally, a connection between Pyk2 activation and the RhoA/ROK pathway leading to MLCP inhibition was established by the demonstration that sodium salicylate prevented both (i) the $K^+$-induced translocation of RhoA from the cytosolic to the particulate fraction (Fig. 14) and (ii) the $K^+$-induced phosphorylation of MYPT1 at the two inhibitory phosphorylation sites (23–25), Thr-697 and Thr-855 (Fig. 15). We also demonstrated that salicylate had no effect on the activity of purified recombinant ROK.

The mechanism whereby Pyk2 activates RhoA remains to be elucidated. Transfection experiments with primary aortic vascular smooth muscle cells in culture have suggested that the guanine nucleotide exchange factor PDZ-RhoGEF may connect activated Pyk2 to RhoA activation via phosphorylation and

activation of its guanine nucleotide exchange factor (GEF) activity (26). This remains to be demonstrated in freshly isolated vascular smooth muscle tissue.

In conclusion, our results support a role for Pyk2 in activation of the RhoA/ROK pathway and $Ca^{2+}$ sensitization in the tonic contractile response of vascular smooth muscle to membrane depolarization. They also emphasize the importance of the development of specific Pyk2 inhibitors as therapeutic agents for the treatment of cardiovascular diseases associated with hypercontractility because up-regulation of the RhoA/ROK pathway has been implicated in the etiology of hypertension (27, 28). This work also extends the regulatory roles of Pyk2 in vascular smooth muscle; Pyk2 was recently implicated in stretch-stimulated growth in the rat portal vein (29).

## REFERENCES


1. Allen, B. G., and Walsh, M. P. (1994) The biochemical basis of the regulation of smooth-muscle contraction. *Trends Biochem. Sci.* **19,** 362–368
2. Bolton, T. B., Prestwich, S. A., Zholos, A. V., and Gordienko, D. V. (1999) Excitation-contraction coupling in gastrointestinal and other smooth muscles. *Annu. Rev. Physiol.* **61,** 85–115
3. Mita, M., Yanagihara, H., Hishinuma, S., Saito, M., and Walsh, M. P. (2002) Membrane depolarization-induced contraction of rat caudal arterial smooth muscle involves Rho-associated kinase. *Biochem. J.* **364,** 431–440
4. Urban, N. H., Berg, K. M., and Ratz, P. H. (2003) $K^+$ depolarization induces RhoA kinase translocation to caveolae and $Ca^{2+}$ sensitization of arterial muscle. *Am. J. Physiol. Cell Physiol.* **285,** C1377–C1385
5. Ratz, P. H., Berg, K. M., Urban, N. H., and Miner, A. S. (2005) Regulation of smooth muscle calcium sensitivity: KCl as a calcium-sensitizing stimulus. *Am. J. Physiol. Cell Physiol.* **288,** C769–C783
6. Mita, M., Tanaka, H., Yanagihara, H., Nakagawa, J., Hishinuma, S., Sutherland, C., Walsh, M. P., and Shoji, M. (2013) Membrane depolarization-induced RhoA/Rho-associated kinase activation and sustained contraction of rat caudal arterial smooth muscle involves genistein-sensitive tyrosine phosphorylation. *J. Smooth Muscle Res.* **49,** 26–45
7. Sutherland, C., and Walsh, M. P. (2012) Myosin regulatory light chain diphosphorylation slows relaxation of arterial smooth muscle. *J. Biol. Chem.* **287,** 24064–24076
8. Takeya, K., Loutzenhiser, K., Shiraishi, M., Loutzenhiser, R., and Walsh, M. P. (2008) A highly sensitive technique to measure myosin regulatory light chain phosphorylation: the first quantification in renal arterioles. *Am. J. Physiol. Renal Physiol.* **294,** F1487-F1492
9. Gong, M. C., Fujihara, H., Somlyo, A. V., and Somlyo, A. P. (1997) Translocation of rhoA associated with $Ca^{2+}$ sensitization of smooth muscle. *J. Biol. Chem.* **272,** 10704–10709
10. Walsh, M. P., Hinkins, S., Dabrowska, R., and Hartshorne, D. J. (1983) Smooth muscle myosin light chain kinase. *Methods Enzymol.* **99,** 279–288
11. Wang, Z., and Brecher, P. (2001) Salicylate inhibits phosphorylation of the nonreceptor tyrosine kinases, proline-rich tyrosine kinase 2 and c-Src. *Hypertension* **37,** 148–153
12. Ying, Z., Giachini, F. R. C., Tostes, R. C., and Webb, R. C. (2009) Salicylates dilate blood vessels through inhibiting PYK2-mediated RhoA/Rho-kinase activation. *Cardiovasc. Res.* **83,** 155–162
13. Han, S., Mistry, A., Chang, J. S., Cunningham, D., Griffor, M., Bonnette, P. C., Wang, H., Chrunyk, B. A., Aspnes, G. E., Walker, D. P., Brosius, A. D., and Buckbinder, L. (2009) Structural characterization of proline-rich tyrosine kinase 2 (PYK2) reveals a unique (DFG-out) conformation and enables inhibitor design. *J. Biol. Chem.* **284,** 13193–13201
14. Walker, D. P., Bi, F. C., Kalgutkar, A. S., Bauman, J. N., Zhao, S. X., Soglia, J. R., Aspnes, G. E., Kung, D. W., Klug-McLeod, J., Zawistoski, M. P., McGlynn, M. A., Oliver, R., Dunn, M., Li, J. C., Richter, D. T., Cooper, B. A., Kath, J. C., Hulford, C. A., Autry, C. L., Luzzio, M. J., Ung, E. J., Roberts, W. G., Bonnette, P. C., Buckbinder, L., Mistry, A., Griffor, M. C., Han, S., and Guzman-Perez, A. (2008) Trifluoromethylpyrimidine-based inhibitors of proline-rich tyrosine kinase 2 (PYK2): structure-activity relationships and strategies for the elimination of reactive metabolite formation. *Bioorg. Med. Chem. Lett.* **18,** 6071–6077
15. Slack-Davis, J. K., Martin, K. H., Tilghman, R. W., Iwanicki, M., Ung, E. J., Autry, C., Luzzio, M. J., Cooper, B., Kath, J. C., Roberts, W. G., and Parsons, J. T. (2007) Cellular characterization of a novel focal adhesion kinase inhibitor. *J. Biol. Chem.* **282,** 14845–14852
16. Allen, J. G., Fotsch, C., and Babij, P. (2010) Emerging targets in osteoporosis disease modification. *J. Med. Chem.* **53,** 4332–4353
17. Dao, P., Jarray, R., Le Coq, J., Lietha, D., Loukaci, A., Lepelletier, Y., Hadj-Slimane, R., Garbay, C., Raynaud, F., and Chen, H. (2013) Synthesis of novel diarylamino-1,3,5-triazine derivatives as FAK inhibitors with anti-angiogenic activity. *Bioorg. Med. Chem. Lett.* **23,** 4552–4556
18. Liu, T.-J., LaFortune, T., Honda, T., Ohmori, O., Hatakeyama, S., Meyer, T., Jackson, D., de Groot J., and Yung, W. K. A. (2007) Inhibition of both focal adhesion kinase and insulin-like growth factor-1 receptor kinase suppresses glioma proliferation *in vitro* and *in vivo*. *Mol. Cancer Ther.* **6,** 1357–1367
19. Golubovskaya, V. M., Nyberg, C., Zheng, M., Kweh, F., Magis, A., Ostrov, D., and Cance, W. G. (2008) A small molecule inhibitor, 1,2,4,5-benzenetetraamine tetrahydrochloride, targeting the Y397 site of focal adhesion kinase decreases tumor growth. *J. Med. Chem.* **51,** 7405–7416
20. Shimada, T., Shimamura, K., and Sunano, S. (1986) Effects of sodium vanadate on various types of vascular smooth muscles. *Blood Vessels* **23,** 113–124
21. Lipinski, C. A., and Loftus, J. C. (2010) The Pyk2 FERM domain: a novel therapeutic target. *Expert Opin. Ther. Targets* **14,** 95–108
22. Kohno, T., Matsuda, E., Sasaki, H., and Sasaki, T. (2008) Protein tyrosine kinase CAK$\beta$/PYK2 is activated by binding $Ca^{2+}$/calmodulin to FERM F2 $\alpha$2 helix and thus forming its dimer. *Biochem. J.* **410,** 513–523
23. Feng, J., Ito, M., Ichikawa, K., Isaka, N., Nishikawa, M., Hartshorne, D. J., and Nakano, T. (1999) Inhibitory phosphorylation site for Rho-associated kinase on smooth muscle myosin phosphatase. *J. Biol. Chem.* **274,** 37385–37390
24. Velasco, G., Armstrong, C., Morrice, N., Frame, S., and Cohen, P. (2002) Phosphorylation of the regulatory subunit of smooth muscle protein phosphatase 1M at Thr850 induces its dissociation from myosin. *FEBS Lett.* **527,** 101–104
25. Murányi, A., Derkach, D., Erdodi, F., Kiss, A., Ito, M., and Hartshorne, D. J. (2005) Phosphorylation of Thr695 and Thr850 on the myosin phosphatase target subunit: inhibitory effects and occurrence in A7r5 cells. *FEBS Lett.* **579,** 6611–6615
26. Ying, Z., Giachini, F. R. C., Tostes, R. C., and Webb, R. C. (2009) PYK2/PDZ-RhoGEF links $Ca^{2+}$ signaling to RhoA. *Arterioscler. Thromb. Vasc. Biol.* **29,** 1657–1663
27. Uehata, M., Ishizaki, T., Satoh, H., Ono, T., Kawahara, T., Morishita, T., Tamakawa, H., Yamagami, K., Inui, J., Maekawa, M., and Narumiya S. (1997) Calcium sensitization of smooth muscle mediated by a Rho-associated protein kinase in hypertension. *Nature* **389,** 990–994
28. Kanda, T., Wakino, S., Homma, K., Yoshioka, K., Tatematsu, S., Hasegawa, K., Takamatsu, I., Sugano, N., Hayashi, K., and Saruta, T. (2006) Rho kinase as a molecular target for insulin resistance and hypertension. *FASEB J.* **20,** 169–171
29. Bhattachariya, A., Turczyńska, K. M., Grossi, M., Nordström, I., Buckbinder L., Albinsson, S., and Hellstrand P. (2014) PYK2 selectively mediates signals for growth versus differentiation in response to stretch of spontaneously active vascular smooth muscle. *Physiol. Rep.* **2,** e12080